

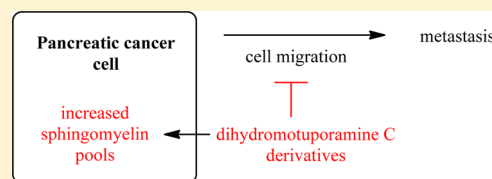
Synthesis and Bioevaluation of Macrocycle–Polyamine Conjugates as Cell Migration Inhibitors

Kristen Skruber, Kelvin J. Chaplin, and Otto Phanstiel, IV*[✉]

University of Central Florida, College of Medicine, 12722 Research Parkway, Orlando, Florida 32826, United States

Supporting Information

ABSTRACT: The motuporamines are natural products isolated from the New Guinea sea sponge *Xestospongia exigua*. Dihydromotuporamine C contains a large macrocycle and an appended polyamine component and was shown to be both antimetastatic and cytotoxic to human L3.6pl pancreatic cancer cells. A series of macrocycle–polyamine conjugates were prepared, and the sequence of the polyamine component was varied to optimize the antimigration properties (as measured in L3.6pl cells) of this molecular class. A one-carbon spacer between the 15-membered carbocycle and the appended polyamine showed improved antimigration properties. A survey of different polyamine sequences containing two, three, or four carbon spacers revealed that the natural polyamine sequence (norspermidine, a 3,3-triamine) was superior in terms of inhibiting the migration of L3.6pl cells in vitro. An investigation of the respective ceramide and sphingomyelin populations in L3.6pl cells revealed that these molecules can modulate both ceramide and sphingomyelin pools in cells and inhibit cell migration.



INTRODUCTION

In 1998, the Andersen group isolated a series of compounds (motuporamines) from the sea sponge *Xestospongia exigua*¹ and showed that they inhibit the invasiveness of MDA-MB-231 breast carcinoma cells in vitro.² The motuporamines have two key structural features, a large macrocycle and a polyamine component.¹ In an attempt to optimize these properties, Andersen et al. synthesized over 40 derivatives of the original isolates and found dihydromotuporamine C (1, Figure 1) to be the most potent.² Derivatization of these isolates included changes to the degree of saturation and size of the macrocyclic ring as well as changes to the polyamine component itself.²

The fact that the motuporamines contain polyamines within their structure may provide a way to target them specifically to cancer cells via the high polyamine import activity often present in human cancers.^{3,4} The native polyamines (putrescine 4h, spermidine 4i, spermine 4j; Figure 2) are low molecular weight aliphatic amines that are positively charged at physiological pH. They are crucial for chromatin condensation, DNA replication, RNA synthesis, and in the translation of mRNA into protein.^{5–7} Polyamines are particularly of interest to the field of oncology, as an increase in intracellular polyamine content is concomitant with the initiation of cancer and is maintained throughout oncogenesis.⁸ The intracellular content of polyamines in cells is under tight control. Polyamines can be biosynthesized from amino acid precursors, as well as imported from the environment via the polyamine transport system (PTS).⁸ Several compounds have been developed to inhibit these key biochemical targets.⁹ For example, difluoromethylornithine (DFMO) is an inhibitor of ornithine decarboxylase (ODC), the rate limiting enzyme in putrescine biosynthesis. However, cancer cells often respond to DFMO therapy by

upregulating import of exogenous polyamines to escape this blockade.¹⁰

The PTS is important in the development and progression of metastatic cancers, as it provides a means to import polyamine metabolites from the tumor microenvironment to maintain the high levels needed for rapidly dividing cells. The PTS has a wide tolerance for ligands,¹¹ which can be leveraged to deliver polyamine vectors tethered to antimetastatic and cytotoxic agents. Therefore, it is possible to selectively target cancer cells via their increased requirement for polyamines and active import processes.¹²

Previously, the Anderson group probed the nature and size of the macrocyclic ring as well as the distance between a 13-membered heterocycle and the tethered polyamine.² This prior work demonstrated that the 15-membered macrocycle provided an improved balance between cytotoxicity and inhibition of invasion of MDA-231 breast cancer cells and the presence of aminopropyl tethers led to improved properties.² The authors did not, however, assess the ability of these materials to target the polyamine transport system. Indeed, alteration of the polyamine motif is a strategy that should improve targeting but only if the polyamine conjugate is recognized by the PTS. Surprisingly, compound 2a showed a significant increase in antimetastatic efficacy but demonstrated no improvement in PTS targeting.¹²

Here we describe the synthesis of additional analogues of the motuporamines. For example by synthesizing longer tether lengths, such as compound 2b, we can further define the relationship between tether length and the antimigration properties of this class of compounds. Other analogues were

Received: August 18, 2017

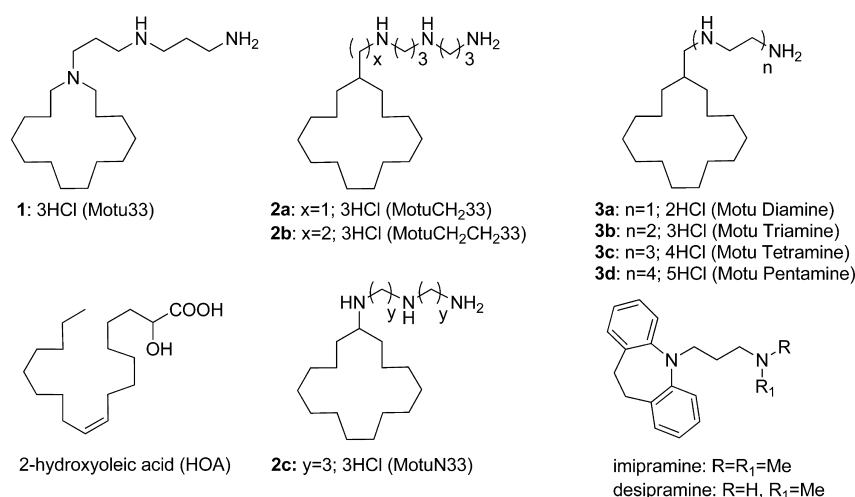


Figure 1. Dihydromotuporamine C (1), synthesized motuporamine derivatives (2a, 2b, and 3), 2-hydroxyoleic acid (a sphingomyelin synthase agonist), imipramine and desipramine (acid sphingomyelinase inhibitors), and MotuN33 (2c).

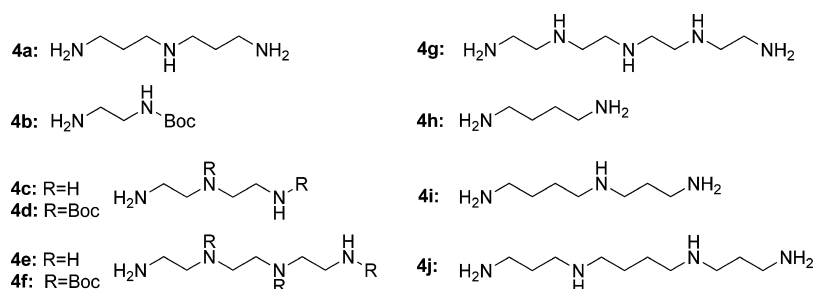
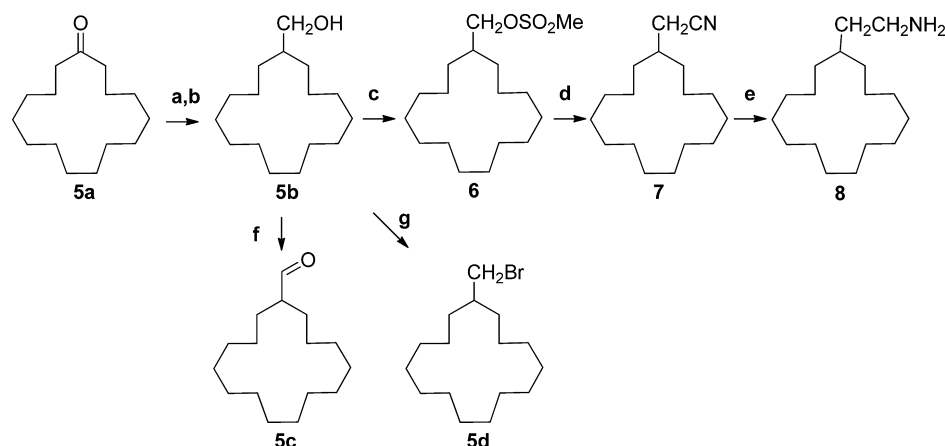


Figure 2. Structures of polyamines. Norspermidine (4a), *tert*-butyl (2-aminoethyl)carbamate (4b), *N*-(2-aminoethyl)ethane-1,2-diamine (4c), *tert*-butyl (2-aminoethyl)(2-((*tert*-butoxycarbonyl)amino)ethyl)carbamate (4d), *N*₁,*N*₁'-(ethane-1,2-diyl)bis(ethane-1,2-diamine) (4e), *tert*-butyl (2-aminoethyl)(2-((*tert*-butoxycarbonyl)(2-((*tert*-butoxycarbonyl)amino)ethyl)amino)ethyl)carbamate (4f), tetraethylene pentaamine (4g), and the native polyamines putrescine (4h), spermidine (4i), and spermine (4j).

Scheme 1^a



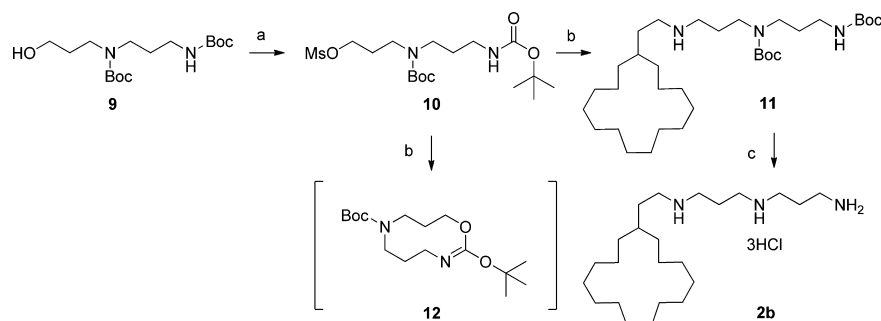
^aReagents and conditions: (a) CH₃PPh₃I, BuLi, THF, 0 °C; (b) BH₃-THF, 0 °C, then, H₂O₂, 3 M NaOH, rt; (c) CH₃SO₂Cl, TEA, 0 °C, then rt; (d) KCN, 18-crown-6, dry CH₃CN, reflux; (e) LiAlH₄, THF, 0 °C, then reflux; (f) PCC, CH₂Cl₂, rt; (g) PBr₃, rt for 1.5 h, then reflux for 1.5 h.

synthesized utilizing ethylene amine motifs (compounds 3a–c) for comparisons. These short polyamine motifs are charge-deficient analogues of the native polyamines and have been shown to interact with established oncogenic targets such as eIF-5a and telomerase.^{13,14} In summary, since the parent 1 and compound 2a were also shown to enhance intracellular sphingomyelin pools,¹² the new analogues described herein were utilized to probe how structural alterations in the

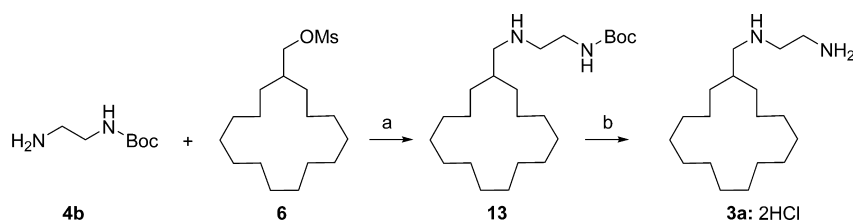
polyamine motif influence PTS targeting, cell migration, and sphingolipid metabolism.

RESULTS AND DISCUSSION

Synthesis. A number of synthetic approaches were investigated using the commercially available ketone cyclopentadecanone 5a (Sigma-Aldrich). The synthesis of the 15-

Scheme 2^a

^aReagents and conditions: (a) TEA, MsCl, 0 °C, then rt overnight; (b) amine 8, Na₂CO₃, rt, 48 h, 20% yield; (c) EtOH, 4 M HCl, 0 °C, then rt.

Scheme 3^a

^aReagents and conditions: (a) CH₃CN, K₂CO₃, 50 °C, 6 days, 12% yield; (b) 4 M HCl, EtOH, rt.

membered macrocycle by Furstner was considered, but it was reported to suffer from low yield.¹⁵ As such, we adopted a strategy that utilized the preformed macrocycle 5a. Our group also developed a multistep pathway for synthesis of the parent compound 1^{16,17} and used ketone 5a and Boc-protected polyamines to make carbocyclic derivatives.¹² This latter approach was facilitated by initial conversion of the ketone to its corresponding alkene followed by anti-Markovnikov addition of borane to give after workup the primary alcohol 5b.¹² From alcohol 5b a number of synthetic routes were attempted to use the alcohol as a platform to create an electrophilic or a nucleophilic reactant. For example, alcohol 5b was previously converted to its corresponding aldehyde 5c in a reaction that unfortunately resulted in low yields.¹² While extended compound 2a could be made from the aldehyde, other chemistries were investigated here in an attempt to improve the yields for extended motuporamine structures with longer tether lengths. In this study, alcohol 5b was converted to extended primary amine 8 which could behave as a nucleophile to attack an electrophilic polyamine scaffold, as shown in Schemes 1 and 2. The alcohol was also readily converted to its bromide 5d through phosphorus tribromide (Scheme 1) for use in Scheme 4.

As shown in Scheme 1, alcohol 5b was converted to its mesylate 6 using methanesulfonyl chloride/TEA in DCM in good yields. Mesylate 6 was then converted to nitrile 7 using 18-crown-6 ether and KCN with a yield of 87%. The resultant nitrile 7 was then reduced to primary amine 8 using lithium aluminum hydride in THF in 49% yield.

The synthesis of 2b was an attempt to further probe the effects of extending the norspermidine “message” away from the macrocycle core by increasing the number of methylene spacers (Scheme 2). Previously, we demonstrated that compound 2a had the best in vivo performance in terms of antimetastatic efficacy in a mouse model of metastatic pancreatic cancer using L3.6pl xenografts.¹² It was hypothesized

that the performance of 2a was predicated upon the increased availability of the polyamine message for its putative receptor; however, 2a had poor PTS targeting.¹² The synthesis of 2b was, therefore, an attempt to understand how further extending this message by increasing the number of methylene spacers (from two to three) would affect PTS targeting and the antimigration properties.

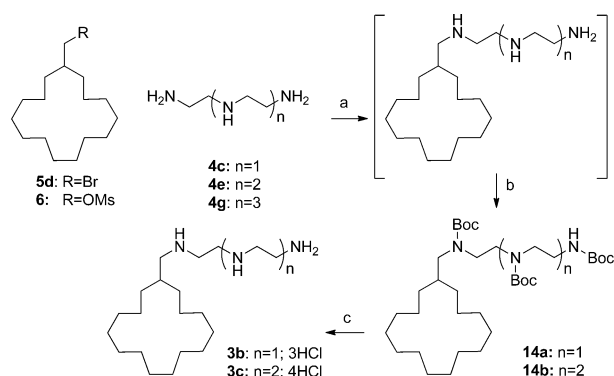
We envisioned synthesis of 2b via the N-alkylation of macrocyclic amine 8 with the electrophilic polyamine component 10. Therefore, a selectively Boc-protected diamine 9 was constructed for this purpose. As shown in Scheme 2, the synthesis of 2b began with the conversion of the Boc-protected polyamine 9 to its corresponding mesylate 10 in 80% yield. The N-alkylation of mesylate 10 with amine 8 was performed in the presence of Na₂CO₃ in DCM and resulted in poor yield of 11 (20%). The low yield in the synthesis of 11 was attributed to the facile formation of a self-cyclized byproduct 12 where (due to the low reactivity of the macrocyclic amine 8) the terminal carbamate group of 10 was observed to react with and displace the appended mesylate group to form byproduct 12. This lowered the amount of 10 available to fully convert 8 to 11 (step b in Scheme 2). Efforts to facilitate this reaction by heating to reflux further increased byproduct formation at the expense of the product 11. A similar conversion of 3-((*tert*-butoxycarbonyl)amino)propyl methanesulfonate to 2-((*tert*-butoxy)-5,6-dihydro-4*H*-1,3-oxazine has been observed by Brown.¹⁸ Nevertheless, the isolated 11 was converted to 2b in 74% yield.

To create the ethylene amine based systems (3a–d), several synthetic strategies were tried. Due to the low yields of 2b and the self-cyclization of the polyamine component, alternative chemistries were investigated that reversed the polarity of the coupling partners so that a nucleophilic polyamine component could be joined to an electrophilic macrocycle. The bulky ketone was very unreactive, and numerous attempts to convert it into other useful functionalities gave very poor yields. For

these reasons, mesylate **6** was selected for coupling to a series of Boc-protected ethylene polyamines (e.g., **4b**, **4d**, and **4f**). Attempts to join **6** with either the Boc-protected triamine **4d** or the Boc-protected tetraamine **4f** failed due to the formation of a self-cyclized byproduct. This was again due to the poor reactivity of the bulky macrocycle, where the polyamine reagent cyclized upon itself likely via urea formation¹⁹ due to the high temperatures and prolonged reaction times needed to drive this reaction forward. Nevertheless, the mono-*N*-Boc diamine **4b** was available commercially (Sigma-Aldrich) and was the only Boc-protected ethylene amine motif to be used successfully in forming the desired structure.

As shown in Scheme 3, the Boc-protected polyamine **4b** was heated with **6** at 50 °C overnight and then for 5 days at reflux (80 °C). The product **13** (53% yield) was separated by column chromatography (7% MeOH/DCM, R_f of **13**: 0.4) from a cyclized urea byproduct that was present in large quantities. Indeed, facile urea formation has been observed in related systems in the presence of base and heat.¹⁹ Subsequent removal of the Boc group with 4 M HCl provided the desired adduct **3a** in high yield but in a disappointing 10% overall yield from **6**. In short, the longer Boc-protected ethylene amine motifs appeared to have poor reactivity and readily displaced their own *tert*-butyl groups to form cyclic ureas in favor of reacting with the mesylate **6**.

To avoid these steric constraints, we devised a “naked” polyamine approach using the free bases of **4c**, **4e**, and **4g** (Scheme 4). This approach was initially not pursued in order to

Scheme 4^a

^aReagents: (a) CH₃CN, K₂CO₃, refluxed 48 h for **14a** and 72 h for **14b**; (b) di-*tert*-butyl dicarbonate, rt; (c) EtOH, 4 M HCl, rt.

avoid reaction of the internal secondary amine(s) with the mesylate, which would form the undesired tertiary amine branched structures instead of the desired linear polyamine architectures. Nevertheless, this naked polyamine approach avoided the possibility of the polyamine portion reacting with an attached Boc group prior to *N*-alkylation. Indeed, the reaction was much more facile without the steric contribution of the *N*-Boc substituents and was successful with **4c** and **4e**, while **4g** was not productive. As shown in Scheme 4, the production of **3b** involved the reaction of triamine **4c** with bromide **5d**. The related derivative **3c** was generated from the reaction of tetraamine **4e** with mesylate **6**. With both **4c** and **4e**, the respective *N*-alkylations were performed in CH₃CN and showed complete disappearance of each starting material after 72 h. After workup, the expected mixture of secondary and tertiary *N*-alkylated products was obtained. These were

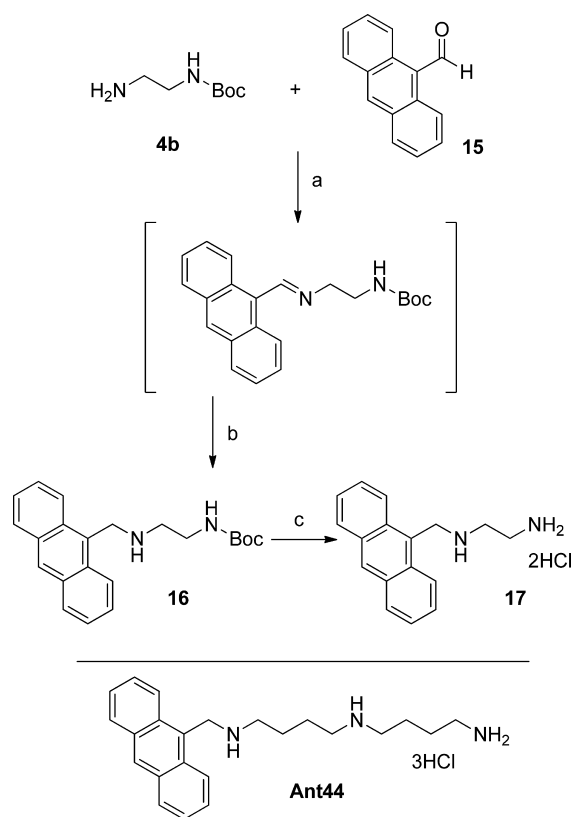
separated by first installing Boc groups at every secondary and primary amine center via excess di-*tert*-butyl dicarbonate. Since the tertiary amine was not *N*-*tert*-butylcarbonylated, the byproduct retained its amine functional group, whereas the desired product was converted to a polycarbamate motif. This change in functional group allowed for easy separation by column chromatography of the undesired tertiary amine byproduct. By use of this approach, a 25% yield was achieved for each of the desired products.

The use of the pentamine **4g** to create **3d** with this method gave a different result. The free base of pentamine **4g** was prepared, and mesylate **6** was added in CH₃CN, refluxed for 72 h, and monitored by ¹H NMR. The mixture was then treated with di-*tert*-butyl dicarbonate, worked up and the crude separated by column chromatography (1% NH₄OH/4.5% MeOH/DCM, R_f suspected product 0.4 and an additional byproduct at R_f = 0.47). This approach was challenging as not all the amine centers were *tert*-butylcarbonylated likely due to steric constraints. Attempts to use Boc-group introduction to drive the reaction to completion resulted in undesired self-cyclization where the secondary amine cyclized back on an existing carbamate group to form a urea linkage. Multiple attempts to separate the product failed, and ultimately the major isolated product appeared to be a cyclized byproduct by NMR and was unresolvable from its upper spot. The crude weight also suggested it was a significantly less productive reaction due to the low conversion of starting material at high temperatures and the long reaction period. Therefore, there were clear limitations to using this unprotected approach for the longer polyamine systems like **4g**. Nevertheless, the method did provide the desired systems **3b** and **3c** (Scheme 4).

*N*¹-Anthracen-9-ylmethylethane-1,2-diamine **17** was generated as a control to evaluate the role of the large *N*-alkyl substituent by comparison to **3a**. Compound **17** was based on prior derivatives, which showed that anthrylpolyamines readily entered cells through the PTS.²⁰ As shown in Scheme 5, the Boc-protected ethylene amine motif **4b** was joined via reductive amination to the commercially available 9-anthraldehyde (Sigma-Aldrich) and resulted in a 75% yield of **17** over three steps via the intermediate imine.

Biological Evaluation. After their syntheses were complete, the compounds were screened for cytotoxicity in Chinese hamster ovary (CHO), CHO-MG (a CHO mutant defective in polyamine transport), and L3.6pl human pancreatic cancer cells. The wild type (wt) CHO cells have high polyamine transport activity and were very sensitive to compounds that exploit the PTS for cell entry. In contrast, the CHO-MG cell line was previously generated by Flintoff et al. via random DNA-alkylation of CHO cells and subsequent cell selection for the ability to survive in the presence of a cytotoxic PTS targeting compound, methylglyoxal bisguanyl hydrazine (MGBG).²¹ The CHO-MG cells have defective polyamine transport and are significantly less sensitive to cytotoxic polyamine compounds.²² L3.6pl cells are hyper-metastatic human pancreatic cancer cells, trained for their ability to migrate from the pancreas to the liver and provide a model of very aggressive pancreatic cancer cells primed for metastasis.²³

Polyamine Transport Selectivity Studies. The CHO (CHO-K1, ATCC) and CHO-MG cell screen uses cytotoxicity measurements to assess transport preference.¹¹ Since the CHO-MG mutant cell line is defective in polyamine transport,²² compounds that selectively enter via the PTS should be less toxic to these cells and give a high CHO-MG IC₅₀ value. In

Scheme 5^a

^aReagents and conditions: (a) 25% MeOH/DCM, rt; (b) NaBH₄, 0 °C, then rt; (c) EtOH, 4 M HCl, rt.

contrast, PTS-dependent compounds should be lethal to wt CHO cells (which have high PTS activity) and give low CHO IC₅₀ values. A ratio of the CHO-MG/CHO IC₅₀ values is then used to assess PTS targeting. A compound that does not enter cells via the PTS should give similar toxicity in both cell lines and an IC₅₀ ratio near 1. In contrast, a compound that targets the PTS should give a high CHO-MG/CHO IC₅₀ ratio.

Compounds **2b**, **2c**, **3a–c**, **5b**, and **17** were tested in the CHO and CHO-MG cell lines at a range of concentrations from 0.1 μM to 100 μM for 48 h in the presence of aminoguanidine (1 mM). Aminoguanidine is an inhibitor of amine oxidases present in calf serum, which readily oxidize amine-containing compounds.¹² As shown in Table 1, the motuporamine derivatives did not target the PTS in CHO cells and gave ratios near 1. In contrast, the N¹-(anthracenylmethyl) homospermidine derivative Ant44²⁰ and diamine **17** gave a CHO-MG/CHO IC₅₀ ratios of 148²⁰ and 5.8, respectively. These findings are consistent with previous studies that showed that the parent compound, dihydromotuporamine C, did not use the PTS for cellular entry.²⁴ The results of this study suggest that the appended aliphatic macrocycle is not conducive for PTS targeting. Indeed, modulation within the polyamine message itself and the distance between the polyamine message and the macrocycle did not improve PTS targeting in this homologous series. For example, we noted that the polyamine message **4b**, when appended to the anthracene substituent (**17**), was able to accomplish modest PTS targeting (CHO-MG/CHO IC₅₀ ratio 5.8) while the related macrocycle-containing compound **3a** did not (CHO-MG/CHO IC₅₀ ratio 0.9).

Table 1. Biological Evaluation of Motuporamine Derivatives on Cytotoxicity in CHO and CHO-MG Cells To Assess PTS Targeting at 48 h^a

compd	IC ₅₀ (μM)		IC ₅₀ ratio CHO-MG/CHO
	CHO-MG	CHO	
1 ^b	2.96 ± 0.10	2.90 ± 0.20	1
2b	2.80 ± 0.11	2.51 ± 0.06	1.1
2c ^b	5.95 ± 0.50	2.84 ± 0.20	2.1
3a	2.37 ± 0.12	2.66 ± 0.11	0.9
3b	2.55 ± 0.07	2.48 ± 0.10	1
3c	2.62 ± 0.13	2.37 ± 0.09	1.1
5b	>100	>100	ND
17	11.33 ± 0.34	1.96 ± 0.11	5.8

^aAll compounds were dosed as aqueous solutions and were compared to a media control with no compound added, except compound **5b**. Compound **5b** was not soluble in water and was dosed in such a manner that the final DMSO concentration was 1% DMSO and was thus compared to a separate 1% DMSO in PBS control with no compound added. For all replicates, *n* = 3. ND = not determined, due to low toxicity of the compound at 100 μM. Note that an anthracenylmethylhomospermidine control (Ant44, bottom in Scheme 5) gave IC₅₀ ratio CHO-MG/CHO of 148.¹⁴ ^bNote that compound **2a** also gave CHO-MG/CHO IC₅₀ ratio of 1.¹⁰

L3.6pl Cytotoxicity Studies. Compounds **2b**, **3a–c**, **5b**, and **17** were tested for cell growth inhibition in human L3.6pl pancreatic cancer cells. The known K-Ras mutation present in this cell line has been shown to correlate with high polyamine uptake due to its ability to affect caveolin-mediated endocytosis,²⁵ which leads to an increase in uptake of polyamine compounds. For this study, L3.6pl cells were treated with a range of compound concentrations (0.1 μM to 100 μM) for 48 h in the presence of aminoguanidine (AG, 250 μM). Prior studies have shown that this amine oxidase inhibitor (AG) was needed to maintain the polyamine compound's potency.¹² Cell viability was evaluated via the tetrazolium compound [3-(4,5-dimethylthiazol-2-yl)-5-(3-carboxymethoxyphenyl)-2-(4-sulfophenyl)-2H-tetrazolium, inner salt (MTS reagent from Promega), and the IC₅ and IC₅₀ values were calculated from the respective plots of % viability versus concentration of compound. Each value represents the concentration of the compound needed to produce the designated level of toxicity (*n* = 3). The IC₅ value is the concentration of the compound that gives 95% viability and represents the dose where minimum toxicity (5% toxicity) from the compound is expected. The IC₅₀ value is the concentration of the compound needed to reduce viability by 50% compared to an untreated control with vehicle (phosphate buffered saline, PBS). The results are shown in Table 2.

The new motuporamine derivatives (**2b**, **3a–c**) displayed sharp cytotoxicity curves (see Supporting Information) with their respective IC₅ values very close to their IC₅₀ concentration and reflect trends observed with other members of this series.^{12,16} Interestingly, the toxicity of the new motuporamine derivatives was not dramatically altered through modulation of the polyamine message. However, the absence of the polyamine component (such as in **5b**) or the addition of an unsaturated anthracene core in place of the aliphatic macrocycle (e.g., **17**) was sufficient to decrease the toxicity. In the case of **17**, PTS targeting was also improved (Table 1). These results suggest that the specific combination of polyamine and macrocycle is responsible for the cytotoxicity of these compounds. We noted

Table 2. Cytotoxicity Evaluation of Motuporamine Derivatives (2b, 3a–c, 5b) and Anthryl Derivative (17) in L3.6pl Cells for 48 h^{a,b}

compd	L3.6pl, 48 h, IC ₅₀ (μM)	L3.6pl, 48 h, IC ₅ (μM)
1 ^b	0.99 ± 0.07	0.60 ± 0.04
2a ^b	89.4 ± 5.4	80.0 ± 4.0
2b	3.34 ± 0.09	1.64 ± 0.09
3a	1.44 ± 0.09	0.6 ± 0.09
3b	1.25 ± 0.05	0.6 ± 0.05
3c	1.64 ± 0.05	0.92 ± 0.05
5b	42.0 ± 3.4	8.4 ± 0.6
17	24.1 ± 1.2	4.15 ± 0.2

^aAll compounds were dosed as aqueous solutions and were compared to a media control with no treatment, except compound 5b. L3.6pl cells were incubated with 250 μM aminoguanidine (AG) for 24 h prior to addition of compound. Compound 5b was not soluble in water and was dosed in such a manner that the final DMSO concentration was 1% DMSO and was thus compared to a 1% DMSO in PBS control with no compound. For all replicates, *n* = 3. ^bReference 12.

that no cell lysis was observed at the IC₅₀ concentrations of these compounds, and direct cell lysis was discarded as a potential mechanism of action for these amphiphilic molecules.

Antimigration Assay. A scratch assay was performed to assess the antimigratory properties of compounds 2b, 3a–c, 5b, and 17 in L3.6pl cells. The parent compound 1 and extended compound 2a were tested as controls,¹² and non-native polyamine motifs 4c and 4e and ethylene diamine HCl were also tested to understand the effect of unsubstituted polyamine structures. It was critical that these cell migration experiments be conducted at compound concentrations that were not toxic to the L3.6pl cells to avoid the interpretation of cell death as migration inhibition. Therefore, the compounds were dosed at the IC₅ value (0.5 μM) of the parent compound 1 to directly compare their potencies at a nontoxic concentration. We also tested them at 1 μM which was close to the MTD of 3b, and some toxicity may be seen at this higher dose. All experiments were run in triplicate and representative microscopy images are shown in their respective figures in the Supporting Information and the numeric results are shown in Table 3.

As mentioned earlier, the Andersen group did not probe the effect of changing the distance between the ring system and the polyamine message. The synthesis of 2a by Muth et al.¹² and 2b here allows for an understanding of the effect of increased distance on cell migration inhibition. Interestingly, antimigration efficacy is retained in compounds 1 and 2a at 0.5 μM, but appears to drop off drastically with the two methylene spacer extension 2b (Table 3).

Compounds 5b and 17 were tested well below their maximum tolerated concentration (IC₅) in order to comment on their efficacy in comparison to the parent compound. Neither control showed any antimigration behavior (see Table 3). Interestingly, the extended system 2b and the macrocyclic alcohol 5b appear to have no antimigration effect at 0.5 μM.

As both compound 2b and the 3a–c series exhibit sharp cytotoxicity curves (Supporting Information), the window between the IC₅ value and IC₅₀ concentration was very small and a dose-limiting toxicity was observed. All compounds were also tested at 1 μM, a concentration that doubles the potency of the parent compound 1. In a similar outcome the efficacy for the ethylene amine based compounds improved at the higher 1

Table 3. Inhibition of L3.6pl Cell Migration by Motuporamine Derivatives (1–3 and 5b), Ethylenediamine and Unsubstituted Polyamines 4c and 4e, and Anthracene Derivative (17)^{a,b,c}

compd (concn)	% cell migration at 24 h ^a	% migration normalized to the control ^a	% migration inhibition compared to control ^a
1% DMSO in PBS control	44.3 ± 2.5		
10% aqueous control	72.3 ± 8.8 ^b		
1 (0.5 μM)	57.4 ± 5.0 ^b	79.4 ± 6.9 ^b	20.6 ± 6.9 ^b
1 (1 μM)	43.6 ± 4.4	60.2 ± 6.6	39.8 ± 6.6
2a (0.5 μM)	57.7 ± 1.6	79.8 ± 6	20.2 ± 6
2a (1 μM)	50.7 ± 6.8	70.1 ± 7.8	29.9 ± 7.8
2b (0.5 μM)	83.5 ± 3.2	115.2 ± 6	−15.5 ± 6
2b (1 μM)	71.2 ± 4.2	98.5 ± 6.5	1.5 ± 6.5
3a (0.5 μM)	67.8 ± 5.6	93.8 ± 7.2	6.2 ± 7.2
3a (1 μM)	53.3 ± 13.0	73.7 ± 10	26.2 ± 10
3b (0.5 μM)	64.9 ± 7.5	89.8 ± 8.2	10.2 ± 8.2
3b (1 μM)	52.9 ± 3.7	73.2 ± 6.3	26.8 ± 6.3
3c (0.5 μM)	67.9 ± 8.2	93.9 ± 8.5	6.1 ± 8.5
3c (1 μM)	60.2 ± 5.5	83.2 ± 7.2	16.8 ± 7.2
ethylenediamine-HCl (1 μM)	100		0
4c (1 μM)	100		0
4e (1 μM)	100		0
5b (1 μM)	60.7 ± 1.6	137.2 ± 2.1	−37.2 ± 2.1
17 (0.5 μM)	67.8 ± 4.0	93.8 ± 6.4	6.2 ± 6.4

^aAll compounds were dosed as aqueous solutions and were compared to the 10% water control, except compound 5b. Compound 5b was not soluble in water and was dosed in DMSO in such a manner that the final DMSO concentration was 1% DMSO and was thus compared to the 1% DMSO in PBS control. For all values *n* = 3 with the exception of those marked otherwise. ^b*n* = 4. ^cL3.6pl cells were incubated for 24 h with 250 μM AG prior to compound addition. For additional details about the antimigration assay, see the Supporting Information. Note that similarly compound 2c was previously reported to inhibit 19.3% (±1.3) of L3.6pl cell migration at 0.6 μM after a 24 h incubation.¹²

μM concentration but did not surpass the antimigration efficacy seen with the parent compound 1.

The unsubstituted non-native ethylene amine motifs (4b, 4c, and 4e) were also assessed for their antimigratory properties via a scratch assay. With incubation of each polyamine for 24 h at 1 μM, however, these compounds showed an increase in migration compared to control and complete wound closure at 24 h. This experiment defines the importance of both the macrocycle (e.g., 5b) and the polyamine (e.g., 4b) for efficacy of these compounds because independently each component is less effective than the conjugate containing both the macrocycle and the amine motif (e.g., 3a).

Sphingolipid Metabolism Modulation. Prior work in yeast suggested that these materials may also affect sphingolipid metabolism.²⁶ Indeed, a heterozygous diploid yeast strain lacking one copy of the genes associated with sphingolipid metabolism (*LCB1* and *TSC10*) was found to be more sensitive to 1 than a wild-type strain.²⁶ Therefore, compounds 1, 2a, and 3c were studied for their ability to modulate sphingolipid and ceramide pools in L3.6pl human pancreatic cancer cells. As shown in Table 4, the parent compound 1 was unique in its ability to increase specific ceramide pools (N16:0 and N24:1) when dosed at 500 nM for 48 h at 37 °C, which may explain its

Table 4. L3.6pl Cell Ceramide Pool Modulation after 48 h Incubation with 500 nM of Each Compound at 37 °C (Expressed in nmol/mg Protein)^a

ceramide species	untreated control	1	2a	3c
N16:0	0.08 ± 0.01	0.17 ± 0.03*	0.11 ± 0.02	0.09 ± 0.01
N24:1	0.37 ± 0.06	0.51 ± 0.03*	0.37 ± 0.03	0.28 ± 0.02
N24:0	0.16 ± 0.04	0.20 ± 0.00	0.14 ± 0.02	0.11 ± 0.03
sum	0.62 ± 0.10	0.89 ± 0.05*	0.63 ± 0.06	0.49 ± 0.06

^aData with asterisk were statistically significant from the untreated control with $p < 0.05$.

high toxicity compared to the other derivatives (see Table 2; 1, IC₅ = 600 nM).¹² In contrast, this ceramide increase was not observed with 2a and 3c at the 500 nM dose.

Compounds 1 and 2a, which were effective antimigration agents at 500 nM (Table 3, ~20% inhibition), significantly increased specific sphingomyelin pools (Table 5). In contrast, compound 3c, which had low antimigration properties at 500 nM (Table 3, ~6% inhibition), resembled the untreated control. As shown in Figure 3 (panel A), the increased sphingomyelin pools can be rationalized by either increased sphingomyelin synthase (SGMS) activity (which generates sphingomyelin from its corresponding ceramide) or inhibition of sphingomyelinase (an enzyme which degrades sphingomyelin to the corresponding ceramide).

In an effort to define the target, we modified a sphingomyelin synthase (SGMS) assay²⁷ and screened the motuporamine derivatives for their possible agonist activity. Since 3c had little effect on sphingomyelin pools, we elected to screen the homologous series 1, 2a, and 2c, which have been previously

reported to affect cell migration (and because 1 and 2a were shown to influence sphingomyelin pools).¹² The SGMS assay utilized a commercially available fluorescently tagged ceramide (NBD-C12-ceramide, Figure 3) as a substrate for the SGMS enzyme present in the whole cell lysates obtained from PanO2 murine pancreatic cancer cells. The results are shown in Figure 4 and quantified in Table 6.

The data in Figure 4 and Table 6 clearly demonstrated that these compounds were not agonists of SGMS, at least under the conditions of our study. An agonist would be expected to increase the SGMS enzyme's ability to convert starting ceramide to sphingomyelin. In addition, one would expect to see an increase in sphingomyelin production in the presence of a SGMS agonist in a dose dependent manner. We observed neither the enhanced production of sphingomyelin nor the expected dose dependence in sphingomyelin production for the three motuporamine derivatives tested: parent 1, 2a, and 2c. In sum, the results obtained with the NBD-C12 ceramide probe (i.e., a fluorescent model of N16:0 ceramide, Figure 3) suggested that SGMS was not the target of motuporamines.

DISCUSSION

Both a norspermidine motif 4a and ethylene amine motifs (4b, 4c, and 4e) were used to synthesize derivatives of dihydromotuporamine C (1). The new derivatives were used to develop structure–activity relationships that relate molecular structure to inhibition of cell migration and their ability to modulate intracellular sphingolipid pools. The original strategy for construction of these motuporamine targets was based on using regioselective Boc-protection of polyamines to maximize formation of linear conjugates between Boc-protected poly-

Table 5. L3.6pl Cell Sphingomyelin Pool Modulation after 48 h Incubation with 500 nM of Each Compound at 37 °C (Expressed in nmol/mg Protein)^a

sphingomyelin species	untreated control	1	2a	3c
N14:0	0.13 ± 0.01	0.14 ± 0.01	0.13 ± 0.01	0.13 ± 0.01
N15:0	0.12 ± 0.00	0.14 ± 0.03	0.13 ± 0.02	0.12 ± 0.01
N16:1	0.28 ± 0.01	0.33 ± 0.02*	0.30 ± 0.01	0.28 ± 0.02
N16:0	2.60 ± 0.06	3.26 ± 0.09**	2.84 ± 0.19	2.66 ± 0.22
N17:0	0.05 ± 0.01	0.06 ± 0.01*	0.06 ± 0.00	0.05 ± 0.01
N18:1	0.07 ± 0.00	0.11 ± 0.01**	0.10 ± 0.00**	0.09 ± 0.01*
N18:0	0.19 ± 0.01	0.32 ± 0.01**	0.27 ± 0.03*	0.24 ± 0.02
N19:0	0.01 ± 0.00	0.01 ± 0.00	0.01 ± 0.00	0.01 ± 0.00
N20:1	0.02 ± 0.00	0.03 ± 0.00**	0.03 ± 0.00*	0.02 ± 0.01
N20:0	0.06 ± 0.01	0.10 ± 0.00*	0.09 ± 0.01**	0.08 ± 0.01*
N21:0	0.03 ± 0.00	0.05 ± 0.00**	0.04 ± 0.00*	0.03 ± 0.00
N22:2	0.01 ± 0.00	0.02 ± 0.00	0.02 ± 0.00	0.02 ± 0.00
N22:1	0.17 ± 0.01	0.27 ± 0.02**	0.22 ± 0.01**	0.19 ± 0.01
N22:0	0.23 ± 0.01	0.35 ± 0.01**	0.31 ± 0.02*	0.28 ± 0.03
N23:2	0.01 ± 0.00	0.01 ± 0.00	0.01 ± 0.00	0.01 ± 0.00
N23:1	0.10 ± 0.00	0.14 ± 0.01**	0.12 ± 0.02*	0.11 ± 0.01
N23:0	0.07 ± 0.00	0.10 ± 0.00**	0.09 ± 0.01*	0.08 ± 0.00*
N24:2	0.30 ± 0.01	0.41 ± 0.02**	0.36 ± 0.02*	0.31 ± 0.03
N24:1	1.07 ± 0.03	1.49 ± 0.04**	1.22 ± 0.06*	1.15 ± 0.14
N24:0	0.32 ± 0.01	0.39 ± 0.01**	0.36 ± 0.02*	0.32 ± 0.03
N25:1	0.02 ± 0.01	0.03 ± 0.00	0.03 ± 0.01	0.02 ± 0.00
N25:0	0.01 ± 0.00	0.03 ± 0.01	0.02 ± 0.01	0.02 ± 0.01
N26:1	0.02 ± 0.00	0.04 ± 0.00**	0.03 ± 0.00	0.03 ± 0.00
sum	5.91 ± 0.11	7.84 ± 0.21**	6.79 ± 0.39 ^b	6.25 ± 0.53

^aAll experiments were performed in triplicate. Data entries with one asterisk ($p < 0.05$) and double asterisk ($p < 0.01$) were compared in a t test (two samples assuming unequal variances, two-tailed) with the untreated control samples. ^b $p = 0.06$.

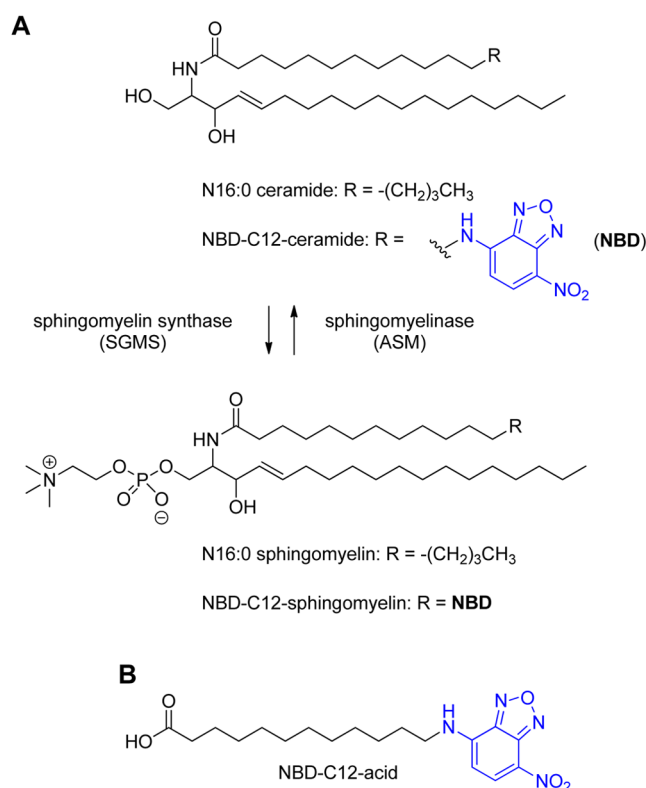


Figure 3. Ceramide and sphingomyelin structures and interconversion pathways: (A) enzymes involved in sphingomyelin–ceramide interconversion and the native and NBD-tagged substrates for these enzymes; (B) structure of NBD-C₁₂ acid, a potential hydrolysis product of NBD-C₁₂-ceramide.

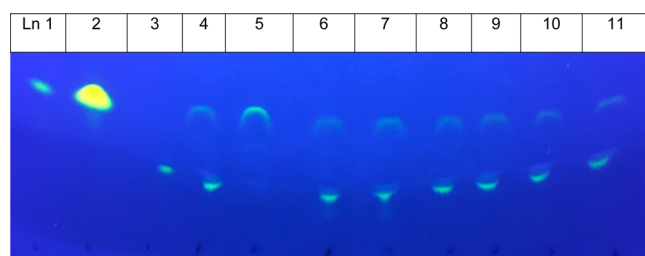


Figure 4. SGMS agonism studies. NBD-C₁₂ ceramide was incubated with PanO2 cell lysates to generate NBD-C₁₂-sphingomyelin in situ in the presence and absence of motuporamine derivatives. TLC was used to separate the NBD-tagged starting ceramide and product sphingomyelin for later analysis by ImageJ (in Table 6). Lane 1: starting material NBD-C₁₂-ceramide. Lane 2: a potential hydrolysis byproduct NBD-C₁₂ acid (12-(7-nitrobenzofurazan-4-ylamino)-dodecanoic acid). Lane 3: product NBD-C₁₂-sphingomyelin. Lane 4: reaction system + deionized water (positive control). Lane 5: reaction system + cell lysis buffer only. Lane 6: reaction system + compound **1** (0.5 μM). Lane 7: reaction system + compound **1** (1 μM). Lane 8: reaction system + compound **2a** (0.5 μM). Lane 9: reaction system + compound **2a** (1 μM). Lane 10: reaction system + compound **2c** (0.5 μM). Lane 11: reaction system + compound **2c** (1 μM). Note that all compounds (**1**, **2a**, and **2c**) were introduced via stock solutions in deionized water.

amines and the 15-membered macrocycle. Surprisingly, we have shown that due to steric issues, this strategy was nonproductive. This is due, in part, to self-cyclization of the Boc-protected polyamines during the prolonged reaction times and high heat needed to drive this coupling step between two bulky starting

Table 6. SGMS Agonism Results for **1**, **2a**, and **2c**^a

compd	concn (μM)	relative % NBD-sphingomyelin produced
untreated	NA	100
1	0.5	89
1	1	75
2a	0.5	88
2a	1	97
2c	0.5	75
2c	1	82

^aThe reaction mixture containing PanO2 cell lysate, NBD-C₁₂-ceramide, and the phosphocholine source were combined and stirred at 37 °C for 3 days. The lipids were then extracted using a 9:1 CHCl₃/MeOH solution and resolved by TLC. The TLC plate was first eluted with 15% MeOH/CHCl₃ (to easily separate the ceramide and sphingomyelin compounds). The plate was then dried under a stream of N₂ gas and re-eluted with 30% MeOH/CHCl₃ to move the sphingomyelin product cleanly off the baseline. The plate was then irradiated with two UV lamps, and an image was captured and analyzed by ImageJ. The relative % NBD-sphingomyelin produced compared to the untreated control was calculated by first subtracting out the background (set by the lysis buffer only negative control) to generate corrected integrated density counts. By use of these corrected values, the respective pixel counts obtained for the NBD-sphingomyelin in each lane were divided by the corrected NBD-sphingomyelin pixel counts obtained in the untreated control (lane 4 in Figure 4) $\times 100$. See the Supporting Information for more detailed information regarding the ImageJ analysis.

materials. In contrast, N-alkylations using naked polyamines (without Boc protection) allowed access to the triamine and tetramine motifs, **3b** and **3c**, albeit in low yield.

The steric hindrance of the bulky 15-membered ring system seems to be a significant determining factor in synthesizing motuporamine derivatives. The 15-membered ketone **5a** was relatively inert to a variety of attempts to convert it to other functional groups. In a similar vein, the low reactivity of polyamine chains containing nearby bulky Boc substituents also severely limited the feasibility of the regioselective strategies employed here. In this regard, the steric demands of the polyamine component were also important determinants of reaction success. Indeed, the “naked” polyamine strategy used here improved the yields of this coupling step. The ethylene amine motifs are shorter than norspermidine and homospermidine, and the decrease in distance between nitrogen centers coupled with the closeness in proximity of Boc groups to the reactive site appears to make this nitrogen-to-carbon coupling reaction especially challenging. Future investigations into synthetic processes that lead to higher yields for these systems are warranted especially for future two carbon polyamine systems based upon **4e**.

The IC₅₀ and PTS targeting determinations for the synthesized compounds showed that the two carbon motuporamine systems **3a–c** were unable to target the PTS and had sharp cytotoxicity curves.^{12,16} The effect of the reduced distance between nitrogen centers had no significant effect on improving potency when appended to the large cyclopentadecane ring. Studies with the macrocycle alcohol **5b** and the unsubstituted polyamines revealed that the individual components were relatively nontoxic. In contrast, the conjugation of the macrocycle and polyamine components was significantly more toxic to cells.

Studies with **3a** and **17** showed that PTS targeting was dependent upon the N-substituent and may require longer

tethers separating bulky N¹-substituents from the polyamine message to improve polyamine recognition by cell surface receptors.

The macrocyclic alcohol **5b** and the unsubstituted non-native ethylene amine motifs (as their respective HCl salts) were all found to be nontoxic and promigratory. While unable to improve upon the potency of **1** at 500 nM to inhibit the migration of L3.6pl cells, compounds **3a–c**, nevertheless, were antimigration compounds, (e.g., see Table 3 for performance of compounds **3a–c** at 1 μ M).

The results obtained suggest that both the polyamine and macrocycle components are required for efficacy as cell migration inhibitors. Indeed, moving the linear triamine message of **1** away from the ring (as performed here with **2a** and **2b**) significantly affected the ability of the compound to block cell migration. While **2a** (containing a methylene spacer) retained the antimigration properties of **1**, this property was lost in compound **2b** (which contains an ethylene spacer). This study shows that efficacy can be significantly altered by minor structural changes in the appended polyamine architecture and suggests that an optimal placement of the appended nitrogen centers is necessary to fully interact with the putative biological target.

We speculated that the observed increased sphingomyelin pools induced by these compounds could be rationalized by either increased sphingomyelin synthase activity or inhibition of sphingomyelinase. Indeed, as shown in Figure 1, the motuporamine derivatives resemble molecules known to interfere with enzymes associated with sphingomyelin–ceramide conversion. For example, 2-hydroxyoleic acid is a known sphingomyelin synthase (SGMS) agonist, where the 2-hydroxyl group and 18-carbon chain length were shown to be critical for this activity.²⁸ We speculated that motuporamine derivatives could mimic this agonist by using the distal polyamine headgroup as a bidentate ligand similar to the α -hydroxycarboxylic acid group in 2-hydroxyoleic acid. In addition, the conformational restriction imparted by the cis alkene in 2-hydroxyoleic acid may be mimicked by the cyclopentadecane ring.

As shown in Figure 4 and Table 6, a SGMS activity assay using a fluorescent C₁₂-ceramide substrate failed to show significant increases in C₁₂-sphingomyelin formation in the presence of these putative SGMS agonists (the motuporamine derivatives) compared to the untreated control. There are several potential interpretations of this result. The most simple conclusion is that the motuporamines are not SGMS agonists. One caveat to this conclusion is that since the motuporamine compounds modulate specific sphingomyelin pools, it is possible that SGMS agonism may be observed using ceramides with other chain lengths (such as C₁₈). Nevertheless, the negative result for SGMS agonistic activity here suggests that the motuporamines likely increase sphingomyelin pools by affecting other pathways. For example, they may inhibit sphingomyelinases like acid sphingomyelinase (ASM).

Indeed, the motuporamines resemble two known functional ASM inhibitors, imipramine and desipramine (Figure 1),²⁹ both of which contain a large macrocycle with 15 atoms along its circumference and an appended amine motif similar to **1**. Future work will investigate whether sphingomyelinases like ASM are inhibited by motuporamines.

Developing molecules, which target cell migration and metastasis, is important because many cancer patients die from metastatic disease. In this regard identifying new scaffolds, which interfere with cell migration and tumor spread, provides

novel starting points for developing antimetastatic medicines for clinical use. We speculate that changes in sphingomyelin pools may affect cell migration via downstream Rho activation and stress fiber formation, outcomes that have both been observed with motuporamines.^{30–32} It remains unclear how these pathways are precisely connected, but we note that released sphingosine 1-phosphate (S1P) can bind to one of five S1P receptors, which in turn lead to differential activation of distinct G-protein responsive pathways including Rho activation.³³ Regardless of mechanism, compound **2a** has been shown to block L3.6pl cell metastasis in vivo.¹²

The ability of motuporamine derivatives to increase intracellular sphingomyelin levels and affect membranes can have broad biomedical applications beyond cancer and metastasis. In fact, we recently described the use of motuporamine derivatives as antimicrobials. We observed that these derivatives can create small leaks in bacterial membranes and can de-energize the bacteria's efflux pump without cell lysis.³⁴ Therefore, future work will also focus on the ability of these compounds to increase the potency of existing antibiotics in drug-resistant microbes as well as inhibit cancer cell migration and alter sphingomyelin pools.

EXPERIMENTAL SECTION

Materials. Silica gel (32–63 μ m) and chemical reagents were purchased from commercial sources and used without further purification. All solvents were distilled prior to use or purchased as analytical grade. All reactions were carried out under atmospheric pressure unless an N₂ atmosphere was specified. ¹H and ¹³C spectra were recorded at 500 or 125 MHz, respectively. TLC solvent systems were listed as volume percentages. All tested compounds provided satisfactory elemental analyses and were tested at \geq 95% purity, with the exception of compound **2b** which was tested at 93% purity.

Biological Studies. CHO (ATCC) and CHO-MG²² as well as L3.6pl cells (RRID: CVCL_0384)²³ were grown in RPMI 1640 medium with the addition of 10% fetal bovine serum and 1% penicillin/streptomycin and grown at 37 °C under a humidified 5% CO₂ atmosphere. CHO and CHO-MG cells were seeded at 10 000 cells/mL, while L3.6pl cells were grown at 5000 cells/mL for cytotoxicity studies and 55 500 cells/mL for antimigration experiments. Cells were treated 24 h prior to compound addition with aminoguanidine (AG, a known inhibitor of polyamine oxidase present in bovine serum) through addition to the growth medium at a concentration of 1 mM for CHO/CHO-MG cells and 250 μ M for L3.6pl cells. The presence of the amine oxidase inhibitor (AG) was important as the compounds tested contained polyamines within their structure and active amine oxidase could cause degradation during the course of the assay.

IC₅₀ Determinations. Cell viability was assessed in sterile 96-well plates (Costar 3599, Corning). After an initial overnight incubation, the respective stock solutions (10 \times) of each compound (10 μ L/well) were added to 90 μ L/well of cell suspension in media with AG (see above). This provided a total volume of 100 μ L in each well. After addition of the compounds, the plates were incubated for 48 h at 37 °C (in a 5% CO₂ atmosphere) and cell viability was assessed via formazan formation (after a 4 h incubation at 37 °C) from the 3-(4,5-dimethylthiazol-2-yl)-5-(3-carboxymethoxyphenyl)-2-(4-sulfenyl)-2H-tetrazolium (MTS) reagent (Promega) via absorbance (490 nm) with a SynergyMx Biotek microplate reader.

Antimigratory Assay. Antimigratory properties were assessed in sterile 96-well plates (Costar 3599, Corning). After an initial 24 h incubation of L3.6pl cell suspension in medium (90 μ L/well) containing 250 μ M AG, a channel was scratched laterally across the plate using a 100 μ L plastic pipet tip. The cells were then washed with PBS (1 \times , 100 μ L) and medium was replaced (90 μ L/well cell suspension in medium with 250 μ M AG) and the respective solution of compound was added (10 μ L/well). Samples were run in

quadruplicate. After 24 h, the cells were imaged (Nikon TE 200) with a 10X objective. To image the same location at two time points, images were taken next to a predrawn line bisecting each well perpendicular to the channel scratched. To standardize each image, all images were cropped in ImageJ software to 700 × 1280 pixels. Cell migration was assessed by measuring the area devoid of cells over a 24 h period and calculated as the following:

$$\begin{aligned} & \% \text{ cell migration at 24 h} \\ & = \frac{(\text{area with no cells at 0 h}) - (\text{area with no cells at 24 h})}{\text{area with no cells at 0 h}} \times 100 \end{aligned}$$

$$\begin{aligned} & \% \text{ cell migration normalized to control} \\ & = \frac{\% \text{ migration with drug at 24 h}}{\% \text{ migration of control at 24 h}} \times 100 \end{aligned}$$

$$\begin{aligned} & \% \text{ cell inhibition at 24 h} \\ & = \left(1 - \frac{\% \text{ migration with drug at 24 h}}{\% \text{ migration of control at 24 h}} \right) \times 100 \end{aligned}$$

SGMS Assay. The assay was used to test for potential agonism of the ceramide to sphingomyelin conversion by the motuporamine compounds **1**, **2a**, and **2c**. The sphingomyelin synthase (SGMS) activity assay was modified from Ding et al.²⁷ Briefly, a cell pellet derived from Pan02 murine pancreatic cancer cells (16 M cells) was lysed using a lysis buffer containing 50 mM Tris-HCl, 1 mM EDTA, 5% sucrose, and protease inhibitors (10 μL/mL of buffer). The cell homogenate was then centrifuged at 5000 rpm for 10 min, and the supernatant was collected and used fresh for the reaction assay. C₁₂-NBD-ceramide (10 μL of 20 μM stock in CHCl₃) and phosphatidylcholine (PC; 10 μL of a 0.1 mg/mL solution comprising 9:1 CHCl₃/MeOH) were pipetted into a 0.6 mL centrifuge tube and concentrated under reduced pressure to provide a tube containing dried residues of both substrates. These were redissolved in a buffer containing 50 mM Tris-HCl (5 μL, pH 7.4) and 25 mM KCl (5 μL). Next, the motuporamine derivative was added (10 μL of either a 2 μM or 4 μM stock in water), and as a final step the cell lysate (20 μL) was added to begin the reaction in a total reaction volume of 40 μL. Note that the 2 μM and 4 μM stock solutions of the motuporamines in deionized water were used to provide final concentrations of 0.5 μM and 1 μM, respectively. A positive control using deionized water (10 μL) in place of the motuporamine stock solution was run to confirm that the cell lysate was responsible for the synthesis of sphingomyelin and not the motuporamine compound. A negative control was run concurrently to confirm that the sphingomyelin synthase contained in the cell lysate was responsible for synthesis of sphingomyelin and not the lysis buffer itself. In this negative control, the reaction was run using lysis buffer only (containing no enzyme). The respective mixtures were incubated at 37 °C for 72 h. Note that an earlier time course study revealed that a 72 h incubation period provided a strong sphingomyelin signal compared to a 24 h experiment (data not shown). The lipids in each reaction mixture were then extracted in the presence of a 2:1 mixture of chloroform/methanol (40 μL), and the chloroform layer containing the unreacted ceramide and sphingomyelin product was carefully separated from the reaction mixture via glass pipet and the organic layer (~25–35 μL obtained) placed into a 0.6 mL microcentrifuge tube. Thin layer chromatography (TLC) used normal phase TLC plates to separate the resulting lipids. Each respective lipid extract (20 μL) was spotted via pipet onto a separate lane on the TLC plate and dried under a stream of nitrogen. The TLC plate was eluted first with 15% MeOH/CHCl₃ until the solvent front reached 90% up the plate (R_f of NBD-C₁₂-ceramide was 0.73). In this solvent system, the sphingomyelin analyte remained at the origin. Therefore, the plate was dried under a stream of nitrogen and re-eluted using the more polar solvent system (30% MeOH/CHCl₃) to elute the sphingomyelin product off the baseline, and elution was stopped before the new solvent front reached the originally eluted NBD C₁₂-ceramide band. This double elution approach provided

nicely defined bands for quantification purposes. Separate controls were run to confirm the elution profile of each analyte using pure NBD-C₁₂-ceramide (Sigma) and NBD-C₁₂-sphingomyelin (Nova). The NBD-C₁₂-acid (lane 2 in Figure 4, a potential hydrolysis product of ceramide that would also contain a NBD tag) was run in parallel to show that it did not interfere with the NBD-C₁₂-sphingomyelin band.

Synthetic Procedures and Characterization. Compounds **1**, **2a**, and **2c** were synthesized previously.¹²

N-(3-Aminopropyl)-N'-(2-cyclopentadecylethyl)propane-1,3-diamine 2b. Compound **11** was dissolved in absolute EtOH (1 mL) and slowly added dropwise to 4 M HCl (1.56 mL) at 0 °C. After the addition was complete, the solution was brought to rt and stirred for 24 h. It was then concentrated under reduced pressure to yield the product **2b** (20 mg, 0.042 mmol, 74% yield). ¹H NMR (D₂O): δ 3.10 (m, 10H, J_{H-H} = 6.1 Hz), 2.09 (m, 4H), 1.58 (m, 2H), 1.45 (m, 1H), 1.29 (s, 28H). ¹³C NMR (CDCl₃): δ 45.9, 43.9, 36.8, 33.7, 33.5, 31.3, 30.9, 30.3, 28.7, 28.1, 27.4, 27.4, 26.5, 25.8, 25.6, 24.0, 23.5. HRMS calcd for C₂₃H₄₉N₃ (M + H) 367.392, found 367.3926. Compound **2b** was 93% pure by HPLC analysis [UV detection at 210 nm showed a major peak eluted (~5 min) on a C₁₈ column using 60% acetonitrile/ aqueous heptanesulfonate buffer at pH 3.8 with a flow rate of 1 mL/min].

N¹-Cyclopentadecylmethylethane-1,2-diamine 3a. Compound **13** (61 mg, 0.16 mmol) was dissolved in EtOH (1 mL), and 4 M HCl/EtOH (1 mL) was added dropwise and stirred at rt overnight. The solvent was then removed under reduced pressure to give a white solid **3a** (50 mg, 0.157 mmol, 98% yield). ¹H NMR (D₂O): δ 3.39 (br s, 4H), 3.01 (br s, 2H), 1.82 (br s, 1H), 1.33 (br s, 28H). ¹³C NMR (D₂O): δ 55.5, 47.3, 38.0, 36.7, 31.8, 29.3, 28.9, 28.6, 26.1. Anal. Calcd for C₁₈H₄₀Cl₂N₂·0.05H₂O: C 60.83, H 11.34, N 7.88. Found: C 61.12, H 11.44, N 7.72.

N-(2-Aminoethyl)-N'-cyclopentadecylmethylethane-1,2-diamine 3b. Compound **14a** (96 mg, 0.153 mmol) was dissolved in solution containing EtOH (3 mL) and 4 M HCl in EtOH (3 mL) and stirred overnight at rt. The solvent was then removed under reduced pressure to give a white solid **3b** (60 mg, 0.138 mmol, 90% yield). ¹H NMR (D₂O): δ 3.45 (m, 8H), 3.02 (br s, 2H), 1.83 (br s, 1H), 1.32 (br s, 28H); ¹³C NMR (D₂O): δ 55.6, 47.1, 46.0, 37.9, 36.7, 31.8, 29.3, 28.94, 28.88, 28.55, 26.1. HRMS for C₂₀H₄₃N₃ (M + H): theory, 325.3439; found, 325.3457. Anal. Calcd for C₂₀H₄₆Cl₃N₃·0.56H₂O: C 53.98, H 10.67, N 9.44. Found: C 54.38, H 10.68 N 9.05.

N-[2-(2-Aminoethylamino)ethyl]-N'-cyclopentadecylmethylethane-1,2-diamine 3c. Removal of the Boc groups of **14b** was performed in 4 M HCl/EtOH by first dissolving **14b** in 200 proof EtOH (5 mL), which required sonication. 4 M HCl in EtOH (5 mL) was then added dropwise while stirring and then stirred overnight. The solvent was then removed under reduced pressure to provide a white solid, **3c** (252 mg, 0.49 mmol, 98% yield). ¹H NMR (D₂O): δ 3.51 (m, 12H), 3.04 (br s, 2H), 1.86 (br s, 1H), 1.33 (s, 28H). ¹³C NMR (D₂O): δ 55.4, 47.1, 46.4, 46.2, 38.0, 36.6, 31.8, 30.5, 29.4, 29.0, 28.8, 26.1. HRMS C₂₂H₄₈N₄ (M + H): theory, 368.3878; found, 368.3879. Anal. Calcd for C₂₂H₅₂Cl₄N₄: C 51.36, H 10.19, N 10.89. Found: C 51.35, H 10.46, N 10.62.

Synthesis of N-(2-Aminoethyl)-N'-[2-(cyclopentadecylmethylamino)ethyl]ethane-1,2-diamine 4f. The free base of 2,2-tetraamine **4c** was generated using N,N'-bis-(2-aminoethyl)-ethane-1,2-diamine (3.00 g, 10.27 mmol, Sigma-Aldrich) with 4 equiv of aq NaOH (1 M, 41 mmol, 41 mL). The water was removed under vacuum, and then the residue was further dried by adding and removing benzene under reduced pressure to remove any excess water. Anhydrous Na₂SO₄ (8 equiv, 82.3 mmol, 11.69 g) was added to a dried vessel with 25% MeOH/CH₂Cl₂ (50 mL). One equivalent of salicylaldehyde (10.27 mmol, 1.10 mL) in MeOH (10 mL) was then added dropwise over 2 h at 0 °C while stirring. Upon addition of the reagent, the reaction immediately turned yellow. Imine formation was monitored by ¹H NMR. After imine formation was complete, the remaining reactive amine centers were reacted with di-*tert*-butyl dicarbonate (3 equiv., 30.87 mmol, 6.74 g) and stirred overnight. The reaction progress was checked by ¹H NMR for full N-bocylation, and additional di-*tert*-butyl dicarbonate was then added (0.3 equiv, 0.67g)

while heating at 40 °C overnight to drive the reaction to completion. The reaction was again checked for *N*-*tert*-butylcarbonylation and confirmed to be complete by NMR. Then MeONH₂·HCl (10.3 mmol, 0.86 g) was added in 1.5 mL of TEA. Note that MeONH₂·HCl was initially not soluble in the TEA, which was used to generate the free base. Upon addition of 25% MeOH/CH₂Cl₂ (5 mL) the methoxyamine easily dissolved and the TEA/MeOH/CH₂Cl₂ solution was then added dropwise to the stirring solution. Imine cleavage was monitored by NMR. Note that an oxime byproduct is formed via methoxyamine exchange with the imine. The MeOH was removed under reduced pressure, and the residue was redissolved in CH₂Cl₂ and washed with saturated Na₂CO₃ (10 mL). The aqueous layer was extracted three times with CH₂Cl₂ and the organic layers were combined and concentrated under reduced pressure to yield a yellow oil (3.65 g). The product was then isolated by column chromatography (1% NH₄OH/10%MeOH/CH₂Cl₂, *R_f*(4f) = 0.65). The product 4f eluted as a light yellow solid (1.48 g, 3.31 mmol, 32% yield). 4f: C₂₁H₄₂N₄O₆. ¹H NMR (CDCl₃): δ 3.31 (br s, 10H), 2.84 (br s, 2H), 1.79 (br s, 2H), 1.46 (br s, 27H). ¹³C NMR (CDCl₃): δ 155.5, 76.6, 46.2, 45.5, 40.2, 39.1, 28.1. HRMS for C₂₁H₄₂N₄O₆ (M + H): theory, 446.3121; found, 446.3104. Anal. Calcd for C₂₁H₄₂N₄O₆·0.2H₂O: C 56.03, H 9.49, N 12.45. Found: C 55.87, H 9.39, N 12.23.

Cyclopentadecylmethanol 5b and Cyclopentadecylcarbaldehyde 5c. Syntheses of 5b and 5c have been described by Muth et al.¹² ¹H NMR analysis matched the literature spectra for these compounds.¹²

Bromomethylcyclopentadecane 5d. The alcohol 5b (250 mg, 1.04 mmol) was placed under an inert atmosphere. Phosphorus tribromide (0.52 mmol, 49 μL) was added by syringe. The reaction immediately turned yellow and started bubbling and was stirred at rt for 1.5 h. Hexane (3 mL) was added, and the reaction was refluxed at 69 °C for another 1.5 h. The reaction turned a brownish yellow color. The vessel was rinsed, and the brown crude (0.48 g) was isolated. Column chromatography (100% *n*-hexane) was performed (with a 30:1 ratio of silica gel/crude) due to the large *R_f* difference (*R_f*(5b) = 0, *R_f*(5d) = 0.8). Visualization of the TLC plate using phosphomolybdic acid and heat provided a convenient monitoring tool. The product 5d was isolated and concentrated under reduced pressure to yield an oil (0.21g, 0.695 mmol, 67% yield). ¹H NMR (CDCl₃): δ 3.38(d, 2H, *J*_{H-H} = 6.1 Hz), 1.72 (m, 1H), 1.38 (br s, 28H). ¹³C NMR (CDCl₃): δ 40.4, 38.7, 31.2, 27.3, 26.9, 26.6, 26.5, 24.6.

Methanesulfonic Acid Cyclopentadecylmethyl Ester 6. Alcohol 5b (998 mg, 4.15 mmol) was added to TEA (643 μL, 4.58 mmol) in CH₂Cl₂. Methanesulfonyl chloride was then added by syringe (355 μL, 4.58 mmol) at 0 °C, and then the solution slowly warmed to rt and stirred overnight. The reaction was monitored by TLC (100% CH₂Cl₂, *R_f*(mesylate 6) = 0.63; *R_f*(alcohol 5b) = 0.37) and then quenched with 1 M NaOH (2 mL). The organic phase was washed three times with 1 M NaOH (5 mL), then separated, dried over anhydrous Na₂SO₄, filtered, and concentrated to give the mesylate 6 as a yellow oil (1.12 g, 3.52 mmol, 85% yield). ¹H NMR (CDCl₃): δ 4.15 (d, 2H, *J*_{H-H} = 6.1 Hz), 3.0 (s, 3H), 1.34 (br s, 29H).

Cyclopentadecylacetonitrile 7. KCN (3.09 g, 47.6 mmol), 18-crown-6 ether (145 mg, 0.48 mmol), and dry CH₃CN (48 mL) were added to mesylate 6 (1.69 g, 5.29 mmol), and the reaction was refluxed overnight. The reaction was monitored by TLC (70% hexanes/CH₂Cl₂, *R_f* = 0.28), and then volatiles were removed under vacuum. The residue was then redissolved in CH₂Cl₂ and washed with water. The layers were separated, and the organic layer was dried over anhydrous Na₂SO₄, filtered, and concentrated to give a yellow crude oil (1.29 g). The crude was then purified by column chromatography (70% hexanes/CH₂Cl₂) to yield a colorless oil (0.92g, 3.69 mmol, 82% yield, 91% conversion). Unreacted mesylate 6 was also recovered as a white crystalline solid (0.15 g, 0.47 mmol, 9% recovery) in (50% hexanes/CH₂Cl₂, *R_f* = 0.3). 7: ¹H NMR δ 2.30 (d, 2H, *J*_{H-H} = 6.6 Hz), 1.80 (m, 1H), 1.34 (br s, 28H). ¹³C NMR: δ 119.2, 33.7, 31.8, 27.1, 26.8, 26.7, 26.6, 26.5, 24.3, 22.9. HRMS for C₁₇H₃₁N (M + H): theory, 250.2535; found, 250.2527. Anal. Calcd for C₁₇H₃₁N: C 81.86, H 12.53, N 5.62. Found: 82.04, 12.63, N 5.51.

2-Cyclopentadecylethanamine 8. Nitrile 7 (412 mg, 1.64 mmol) was dissolved in dry THF (5 mL, 55.5 mmol) and added dropwise to a stirred solution of LiAlH₄ (207 mg, 5.46 mmol) in THF (5 mL) at 0 °C. The reaction was then warmed to rt and refluxed overnight. The reaction was monitored for the disappearance of the nitrile with TLC (1% NH₄OH/15% MeOH/CH₂Cl₂, *R_f*(8) = 0.28, *R_f*(7) = 0.55). After disappearance of the starting material was confirmed by TLC, the reaction mixture was concentrated and redissolved in CH₂Cl₂. The organic phase was washed with a solution of water (0.9 mL) and 5 M NaOH (0.15 mL), and the organic layer was separated, dried over anhydrous Na₂SO₄, filtered, and concentrated under reduced pressure to yield a colorless oil. Column chromatography (85% CH₂Cl₂, 15% methanol, 1% NH₄OH) provided amine 8 (203 mg, 0.80 mmol, 49% yield). ¹H NMR: δ 2.72 (m, 2H), 1.41 (m, 4H), 1.34 (m, 28H). ¹³C NMR: δ 40.0, 38.9, 34.2, 32.4, 27.6, 26.9, 26.6. HRMS for C₁₇H₃₅N (M + H): theory, 253.2789; found, 253.2770. Anal. Calcd for C₁₇H₃₅N·0.2H₂O: C 79.43, H 13.88, N 5.45. Found: C 79.24, H 13.94, N 5.37.

Methanesulfonic Acid 3-[*tert*-Butoxycarbonyl-(3-*tert*-butoxycarbonylamino)propyl]amino]propyl Ester 10. (3-*tert*-Butoxycarbonylamino)propyl-(3-hydroxypropyl)carbamic acid *tert*-butyl ester 9¹⁶ (100 mg, 0.3 mmol) was added to TEA (127 μL, 0.9 mmol) and CH₂Cl₂ (3 mL). Methanesulfonyl chloride (34.9 μL, 0.45 mmol) was added dropwise at 0 °C via syringe under a nitrogen atmosphere. Once the addition was complete, the syringe was rinsed with CH₂Cl₂ (0.6 mL). The reaction progress was monitored by TLC (5% MeOH/CH₂Cl₂, *R_f*(alcohol) = 0.25; *R_f*(mesylate) = 0.37). After 24 h, 4 M NaOH (5 mL) was added with stirring. The organic layer was separated, dried over anhydrous Na₂SO₄, filtered, and concentrated under reduced pressure to yield mesylate 10 (99 mg, 0.24 mmol, 80% yield).

9: ¹H NMR (CD₃OD) δ 3.55 (t, 2H), 3.28 (t, 2H), 3.24 (t, 2H), 3.04 (q, 2H), 1.62–1.81 (m, 4H), 1.44 (s, 9H), 1.42 (s, 9H).¹⁶

10: ¹H NMR (CDCl₃) δ 4.25 (t, 2H, *J*_{H-H} = 6.2 Hz), 3.28 (br s, 4H), 3.11 (br s, 2H), 3.02 (s, 3H), 1.99 (m, 2H), 1.67 (m, 2H), 1.56 (s, 3H), 1.47 (s, 9H), 1.44 (m, 9H)

(3-*tert*-Butoxycarbonylamino)propyl-[3-(2-cyclopentadecylethylamino)propyl]carbamic Acid *tert*-Butyl Ester 11. 2-Cyclopentadecylethylamine 8 (0.07g, 0.28 mmol) was dissolved in CH₂Cl₂ and added to Na₂CO₃ (75 mL, 1.79 mmol) while stirring at rt. Di-Boc mesylate 10 (121 mg, 0.296 mmol) was dissolved in CH₂Cl₂ (1 mL) and added to the solution dropwise. The reaction was stirred for 48 h and was monitored by TLC (10% MeOH/CH₂Cl₂; *R_f* = 0.34). After the reaction was complete, CH₂Cl₂ (2 mL) was added and the solution was washed three times with aq Na₂CO₃ (10% by w/v, 3 mL). The organic layer was separated, dried over anhydrous Na₂SO₄, filtered, and concentrated under reduced pressure to yield a crude yellow oil (248 mg). Column chromatography (10% MeOH/CH₂Cl₂, followed by 10% MeOH/1% NH₄OH, CH₂Cl₂) provided a product mixture as a clear oil (60 mg, 0.106 mmol, 38% yield) with 11 along with a self-cyclized starting material 12. These were then separated by running a second column (4.5% MeOH/CH₂Cl₂) to yield the byproduct 12 (27.3 mg, 0.0572 mmol, 21% yield) and the desired product 11 (32 mg, 0.056 mmol, 20% yield) as a yellow oil.

11: ¹H NMR (CDCl₃) δ 3.31(br s, 2H), 3.16 (br s, 2H), 3.03 (br s, 2H), 2.84 (br s, 4H), 2.06 (m, 2H), 1.65 (m, 4H), 1.40 (s, 18H), 1.36 (br s, 29H). ¹³C NMR: δ 46.9, 45.0, 37.8, 34.6, 32.4, 31.3, 29.7, 29.1, 28.3, 27.5, 26.8, 26.6, 26.5, 25.0, 24.3, 22.7. HRMS for C₃₃H₆₅Cl₃N₃O₄ (M + H): theory, 567.4973; found, 567.4975.

12: ¹H NMR (CDCl₃) δ 4.25 (m, 2H), 3.30 (br s, 4H), 3.11 (s, 2H), 2.0 (m, 2H), 1.66 (m, 2H), 1.46 (s, 18H).

[2-(Cyclopentadecylmethylamino)ethyl]carbamic Acid *tert*-Butyl Ester 13. The commercially available ((2-aminoethyl)carbamic acid *tert*-butyl ester 4b (286 mg, 1.78 mmol, Sigma) was added to mesylate 6 (508 mg, 1.59 mmol) in CH₃CN (20 mL) with K₂CO₃ (0.72 g) at 50 °C. After 5 days the reaction showed 50% conversion, and most of the CH₃CN was stripped off (leaving 5 mL) and heated overnight for complete conversion. The solvent was removed under reduced pressure, redissolved in DCM, and washed with water. The crude (620 mg) was then purified by column chromatography (7%

MeOH/DCM R_f (**13**) = 0.4) to give **13** as a clear oil (75 mg, 0.196 mmol, 12% yield) as well as a large amount of what appeared to be a cyclized urea byproduct (250 mg). **13**: ^1H NMR (CD_4O) δ 3.23 (broad s, 2H), 2.78 (br s, 2H), 2.60 (br s, 2H), 1.63 (s, 1H), 1.45 (s, 9H), 1.37 (br s, 28H). ^{13}C NMR (CD_4O): δ 150.8, 68.0, 50.4, 31.9, 28.9, 28.2, 28.0, 27.9, 27.8. HRMS for $\text{C}_{23}\text{H}_{46}\text{N}_2\text{O}_2$ ($\text{M} + \text{H}$): theory, 382.3558; found, 382.3559. Anal. Calcd for $\text{C}_{23}\text{H}_{46}\text{N}_2\text{O}_2 \cdot 0.3\text{H}_2\text{O}$: C 71.19, H 12.10, N 7.22. Found: C 71.02, H 12.05, N 7.20.

(2-tert-Butoxycarbonylaminoethyl)-[2-(tert-butoxycarbonyl-cyclopentadecylmethylamino)ethyl]carbamic Acid tert-Butyl Ester 14a. Triamine **4c** (N^1 -(2-aminoethyl)ethane-1,2-diamine, 255 mg, 2.47 mmol, Sigma) was added dropwise to bromide **5d** (250 mg, 0.82 mmol) in CH_3CN (3 mL) along with K_2CO_3 (1.17 g, 8.47 mmol) at rt, and then the mixture was refluxed for 48h. After 48 h, ^1H NMR showed complete disappearance of starting material and the reaction was concentrated and resuspended in DCM and washed with 0.1 M NaOH. The organic layer was separated, dried over anhydrous Na_2SO_4 , filtered, and concentrated to give a light yellow oil (272 mg). Di-tert-butyl dicarbonate was added (540 mg, 2.47 mmol) in 25% MeOH/DCM (10 mL) at 40 °C and the reaction stirred overnight. Bocylation was assessed by ^1H NMR, and when complete, the reaction was concentrated, redissolved in DCM, and washed with aq Na_2CO_3 . The organic layer was separated, dried over anhydrous sodium sulfate, filtered, and concentrated under reduced pressure to give a yellow oil (706 mg). The crude was then purified by column chromatography (2% MeOH/DCM R_f (**14a**) = 0.4) to give **14a** as a viscous yellow oil (154 mg, 25% yield). ^1H NMR (CDCl_3): δ 3.30 (m, 8H), 3.06 (m, 2H), 3.04 (m, 1H), 1.68 (s, 1H), 1.45 (s, 27H), 1.31 (br s, 28H). ^{13}C NMR (CDCl_3): δ 155.9, 79.9, 52.5, 46.7, 45.5, 39.8, 36.2, 30.2, 28.4, 26.8, 24.4. HRMS for $\text{C}_{35}\text{H}_{67}\text{N}_3\text{O}_6$ ($\text{M} + \text{H}$): theory, 625.5043; found, 625.5030. Anal. Calcd for $\text{C}_{35}\text{H}_{67}\text{N}_3\text{O}_6$: theory, C 67.16, H 10.79, N 6.71. Found: C 67.42, H 10.92, N 6.63.

[2-(tert-Butoxycarbonyl-(2-[tert-butoxycarbonyl-(2-tert-butoxycarbonylaminoethyl)amino)ethyl]amino)ethyl]-cyclopentadecylmethylcarbamic Acid tert-Butyl Ester 14b. Triethylene tetraamine tetrahydrochloride ($\text{N,N}'$ -bis(2-aminoethyl)-ethane-1,2-diamine, Sigma) (1.0 g, 3.42 mmol) was dissolved in 1 M NaOH (13.8 mL) to give the free tetraamine base **4e**. The water was then removed under vacuum and benzene added to the residue and removed under vacuum to facilitate trace water removal (via benzene-water azeotrope) to give "dry" **4e**. Mesylate **6** (628 mg, 2 mmol) was dissolved in CH_3CN with K_2CO_3 (391 mg, 2.83 mmol), and the reaction showed complete conversion after 72 h at 50 °C by ^1H NMR. The reaction was concentrated to provide a residue, which was dissolved in DCM and washed with 0.1 M NaOH (30 mL). A difficult emulsion ensued. The organic layer was separated, dried over anhydrous Na_2SO_4 , filtered, and concentrated to give organic layer no. 1. The remaining emulsion/aqueous layer was concentrated and redissolved in DCM at a lower temperature, and any remaining precipitates were filtered off. The precipitates were washed with DCM and the organic filtrate was pooled with organic layer no. 1 and they were collectively concentrated to give a yellow viscous oil (806 mg). The crude oil was redissolved in 25% MeOH/DCM and reacted with di-tert-butyl dicarbonate (8.75 mmol, 1.91 g). The reaction was monitored for bocylation by ^1H NMR and then worked up using saturated aq Na_2CO_3 and DCM. The organic layer was separated, dried over anhydrous Na_2SO_4 , filtered, and concentrated to give a yellow oil (1.57 g). Column chromatography (25% EtOAc/hexanes, R_f (**14b**) = 0.39) gave **14b** as a viscous oil (383 mg, 0.5 mmol, 25% yield). ^1H NMR (CDCl_3): δ 3.32 (m, 12H), 3.08 (br s, 1H), 3.03 (br s, 2H), 1.46 (s, 36H), 1.33 (br s, 29H). ^{13}C NMR (CDCl_3): δ 155.4, 80.2, 79.4, 51.7, 45.4, 36.1, 35.8, 36.1, 35.8, 30.2, 28.5, 26.8, 26.4, 24.4. HRMS $\text{C}_{42}\text{H}_{80}\text{N}_4\text{O}_8$ ($\text{M} + \text{H}$): theory, 768.5987; found, 768.5976. Anal. Calcd $\text{C}_{42}\text{H}_{80}\text{N}_4\text{O}_8$: C 65.59, H 10.48, N 7.28. Found: C 65.89, H 10.64, N 7.26.

N^1 -Anthracen-9-ylmethylethane-1,2-diamine 17. To a stirred solution of mono-Boc-diamine **4b** (268 mg, 1.67 mmol) in 25% methanol/DCM (10 mL) was added a solution of 9-anthraldehyde (289 mg, 1.40 mmol) in 5 mL of 25% methanol/DCM under N_2 . The solution was allowed to stir at rt overnight until imine formation was

complete (monitored by ^1H NMR). The solvent was removed in vacuo and the crude imine was redissolved in 50% methanol/DCM and cooled to 0 °C. NaBH_4 (167 mg, 4.28 mmol) was added, and the mixture was stirred at rt overnight. The solvents were removed under vacuum, and the residue was redissolved in DCM and washed with saturated Na_2CO_3 . The organic layer was separated, dried over anhydrous Na_2SO_4 , filtered, and concentrated to give a solid (521 mg crude) which was purified by 5% MeOH/ CHCl_3 to yield 412 mg (1.18 mmol) of adduct **16** (80% yield). Debocylation with 2 mL of ethanol and 2 mL of 4 M HCl gave **17** as its dihydrochloride salt (340 mg, 1.05 mmol, 89% yield) for an overall yield of 75%. ^1H NMR (D_2O): δ 8.40 (s, 1H), 8.05 (m, 2H), 7.63 (m, 2H), 7.53 (m, 2H), 4.95 (s, 2H), 3.55 (m, 2H), 3.35 (m, 2H). ^{13}C NMR (25% DMSO- d_6 in D_2O): δ 133.4, 132.8, 131.9, 130.3, 128.3, 125.4, 124.3, 47.3, 46.0, 38.3. Anal. Calcd $\text{C}_{17}\text{H}_{20}\text{N}_2\text{Cl}_2 \cdot 0.3\text{H}_2\text{O}$: C 62.13, H 6.32, N 8.52. Found: C 62.10, H 6.19, N 8.47.

■ ASSOCIATED CONTENT

📄 Supporting Information

The Supporting Information is available free of charge on the ACS Publications website at DOI: [10.1021/acs.jmedchem.7b01222](https://doi.org/10.1021/acs.jmedchem.7b01222).

Sample cytotoxicity curves for **3a–c** with L3.6pl cells, additional scratch assay protocol details, representative scratch assay images using a non-native polyamine as well as ^1H and ^{13}C NMR spectra for compounds **2b**, **3a–c**, **4f**, **5d**, **6** (^1H only), **7**, **8**, **10** (^1H only), **11**, **12** (^1H only), **13**, **14a**, **14b**, **16**, and **17**, and more information regarding the ImageJ analysis (PDF)

Molecular formula strings and some data (CSV)

■ AUTHOR INFORMATION

✉ Corresponding Author

*E-mail: otto.phanstiel@ucf.edu. Phone: 407-823-6545. Fax: 407-384-2062.

ORCID

Otto Phanstiel IV: [0000-0001-7101-1311](https://orcid.org/0000-0001-7101-1311)

Notes

The authors declare no competing financial interest.

■ ACKNOWLEDGMENTS

The authors thank the 2011 Department of Defense Congressionally Directed Medical Research Program (CDMRP) Peer Review Cancer Research Program (PRCRP) Discovery Award CA110724 and the UCF College of Medicine for financial support of this research and Dr. Isaiah Fidler at the University of Texas M. D. Anderson Cancer Center and Dr. Wayne Flintoff at the University of Western Ontario for their generous gifts of L3.6pl and CHO-MG cells, respectively, for this research. We also acknowledge the assistance of Dr. Julia Soulakova and Bee Ben Khallouq at UCF-COM with the statistical analyses and John Reyenga for his assistance in developing the synthetic methods to access compound **10**.

■ ABBREVIATIONS USED

AG, aminoguanidine; ASM, acid sphingomyelinase; Boc, tert-butylcarbonyl; CHO, Chinese hamster ovary; CHO-MG, Chinese hamster ovary cell defective in polyamine transport; DCM, dichloromethane; DFMO, difluoromethylornithine; DMSO, dimethylsulfoxide; MGBG, methylglyoxal bisguanyl hydrazine; MTS, 3-(4,5-dimethylthiazol-2-yl)-5-(3-carboxymethoxyphenyl)-2-(4-sulfophenyl)-2H-tetrazolium, inner salt; NBD, nitrobenzoxadiazole; ODC, ornithine

decarboxylase; PBS, phosphate buffered saline; PC, phosphatidylcholine; PCC, pyridinium chlorochromate; PTS, polyamine transport system; S1P, sphingosine 1-phosphate; SGMS, sphingomyelin synthase; TEA, triethylamine

REFERENCES

- (1) Williams, D. E.; Lassota, P.; Andersen, R. J. Motuporamines A-C, cytotoxic alkaloids isolated from the marine sponge *Xestospongia exigua* (Kirkpatrick). *J. Org. Chem.* **1998**, *63*, 4838–4841.
- (2) Williams, D. E.; Craig, K. S.; Patrick, B.; McHardy, L. M.; van Soest, R.; Roberge, M.; Andersen, R. J. Motuporamines, anti-invasion and anti-angiogenic alkaloids from the marine sponge *Xestospongia exigua* (Kirkpatrick): Isolation, structure elucidation, analogue synthesis, and conformational analysis. *J. Org. Chem.* **2002**, *67*, 245–258.
- (3) Muth, A.; Kamel, J.; Kaur, N.; Shicora, A. C.; Ayene, I. S.; Gilmour, S. K.; Phanstiel, O. Development of polyamine transport ligands with improved metabolic stability and selectivity against specific human cancers. *J. Med. Chem.* **2013**, *56* (14), 5819–5828.
- (4) Madan, M.; Patel, A.; Skrubber, K.; Geerts, D.; Altomare, D. A.; Phanstiel, O. ATP13A3 and caveolin-1 as potential biomarkers for difluoromethylornithine-based therapies in pancreatic cancers. *Am. J. Cancer Res.* **2016**, *6*, 1231–1252.
- (5) Saini, P.; Eyler, D. E.; Green, R.; Dever, T. E. Hypusine-containing protein eIF5A promotes translation elongation. *Nature* **2009**, *459* (7243), 118–121.
- (6) Hoopes, B. C.; McClure, W. R. Studies on the selectivity of DNA precipitation by spermine. *Nucleic Acids Res.* **1981**, *9* (20), 5493–5504.
- (7) Park, M. H. The post-translational synthesis of a polyamine-derived amino acid, hypusine, in the eukaryotic translation initiation factor 5A (eIF5A). *J. Biochem.* **2006**, *139* (2), 161–169.
- (8) Palmer, A. J.; Wallace, H. M. The polyamine transport system as a target for anticancer drug development. *Amino Acids* **2010**, *38* (2), 415–422.
- (9) Meyskens, F. L., Jr.; Gerner, E. W. Development of difluoromethylornithine (DFMO) as a chemoprevention agent. *Clin. Cancer Res.* **1999**, *5* (5), 945–951.
- (10) Seiler, N. Thirty years of polyamine-related approaches to cancer therapy. Retrospect and prospect. Part I. Selective enzyme inhibitors. *Curr. Drug Targets* **2003**, *4* (7), 537–564.
- (11) Seiler, N.; Delcros, J. G.; Moulinoux, J. P. Polyamine transport in mammalian cells. An update. *Int. J. Biochem. Cell Biol.* **1996**, *28* (8), 843–861.
- (12) Muth, A.; Pandey, V.; Kaur, N.; Wason, M.; Baker, C.; Han, X.; Johnson, T. R.; Altomare, D. A.; Phanstiel, O. Synthesis and biological evaluation of antimetastatic agents predicated upon dihydromotuporamine C and its carbocyclic derivatives. *J. Med. Chem.* **2014**, *57* (10), 4023–4034.
- (13) Hyvonen, M. T.; Ucal, S.; Pasanen, M.; Peraniemi, S.; Weisell, J.; Khomutov, M.; Khomutov, A. R.; Vepsalainen, J.; Alhonen, L.; Keinanen, T. A. Triethylenetetramine modulates polyamine and energy metabolism and inhibits cancer cell proliferation. *Biochem. J.* **2016**, *473* (10), 1433–1441.
- (14) Liu, J.; Guo, L.; Yin, F.; Zheng, X.; Chen, G.; Wang, Y. Characterization and antitumor activity of triethylene tetramine, a novel telomerase inhibitor. *Biomed. Pharmacother.* **2008**, *62* (7), 480–485.
- (15) Furstner, A.; Rumbo, A. Ring-closing alkyne metathesis. Stereoselective synthesis of the cytotoxic marine alkaloid motuporamine C. *J. Org. Chem.* **2000**, *65*, 2608–2611.
- (16) Kaur, N.; Delcros, J.-G.; Martin, B.; Phanstiel, O. Synthesis and biological evaluation of dihydromotuporamine derivatives in cells containing active polyamine transporters. *J. Med. Chem.* **2005**, *48*, 3832–3839.
- (17) Breitbeil, F.; Kaur, N.; Delcros, J.-G.; Martin, B.; Abboud, K. A.; Phanstiel, O. Modeling the preferred shapes of polyamine transporter ligands and dihydromotuporamine-C mimics: Shovel versus hoe. *J. Med. Chem.* **2006**, *49*, 2407–2416.
- (18) Brown, M. J. Synthesis, Structure and Functionalisation of 1,2-Diazetidines. Ph.D. Dissertation, Department of Chemistry, University of Warwick, Coventry, U.K. CV47AL, 2011, (Order No. US68598). Available from ProQuest Dissertations & Theses A&I; ProQuest Dissertations & Theses Global (1033192588) (Order No. US68598). Retrieved from <https://login.ezproxy.net.ucf.edu/login?url=https://search.proquest.com/docview/1033192588?accountid=10003>.
- (19) Kutovaya, I. V.; Shmatova, O. I.; Tkachuk, V. M.; Melnichenko, N. V.; Vovk, M. V.; Nenajdenko, V. G. Aza-Henry reaction with CF₃-Ketimines: An efficient approach to trifluoromethylated-nitroamines, 1,2-diamines, -aminoximes, and imidazolidinones. *Eur. J. Org. Chem.* **2015**, *2015* (30), 6749–6761.
- (20) Phanstiel, O., IV; Kaur, N.; Delcros, J.-G. Structure-activity investigations of polyamine-anthracene conjugates and their uptake via the polyamine transporter. *Amino Acids* **2007**, *33*, 305–313.
- (21) Heaton, M. A.; Flintoff, W. F. Methylglyoxal-bis-(guanylylhydrazone)-resistant Chinese hamster ovary cells: Genetic evidence that more than a single locus controls uptake. *J. Cell. Physiol.* **1988**, *136*, 133–139.
- (22) Mandel, J. L.; Flintoff, W. F. Isolation of mutant mammalian cells altered in polyamine transport. *J. Cell. Physiol.* **1978**, *97*, 335–344.
- (23) Bruns, C. J.; Harbison, M. T.; Kuniyasu, H.; Eue, I.; Fidler, I. J. In vivo selection and characterization of metastatic variants from human pancreatic adenocarcinoma by using orthotopic implantation in nude mice. *Neoplasia* **1999**, *1* (1), 50–62.
- (24) Muth, A.; Madan, M.; Archer, J. J.; Ocampo, N.; Rodriguez, L.; Phanstiel, O. Polyamine transport inhibitors: design, synthesis, and combination therapies with difluoromethylornithine. *J. Med. Chem.* **2014**, *57* (2), 348–363.
- (25) Roy, U. K.; Rial, N. S.; Kachel, K. L.; Gerner, E. W. Activated K-RAS increases polyamine uptake in human colon cancer cells through modulation of caveolar endocytosis. *Mol. Carcinog.* **2008**, *47* (7), 538–553.
- (26) Sturgeon, C. M.; Kemmer, D.; Anderson, H. J.; Roberge, M. Yeast as a tool to uncover the cellular targets of drugs. *Biotechnol. J.* **2006**, *1* (3), 289–298.
- (27) Ding, T.; Li, Z.; Hailemariam, T.; Mukherjee, S.; Maxfield, F. R.; Wu, M. P.; Jiang, X. C. SMS overexpression and knockdown: impact on cellular sphingomyelin and diacylglycerol metabolism, and cell apoptosis. *J. Lipid Res.* **2008**, *49* (2), 376–385.
- (28) Barcelo-Coblijn, G.; Martin, M. L.; de Almeida, R. F.; Noguera-Salva, M. A.; Marcilla-Etxenike, A.; Guardiola-Serrano, F.; Luth, A.; Kleuser, B.; Halver, J. E.; Escriba, P. V. Sphingomyelin and sphingomyelin synthase (SMS) in the malignant transformation of glioma cells and in 2-hydroxyoleic acid therapy. *Proc. Natl. Acad. Sci. U. S. A.* **2011**, *108* (49), 19569–19574.
- (29) Kornhuber, J.; Tripal, P.; Reichel, M.; Terfloth, L.; Bleich, S.; Wiltfang, J.; Gulbins, E. Identification of new functional inhibitors of acid sphingomyelinase using a structure-property-activity relation model. *J. Med. Chem.* **2008**, *51*, 219–237.
- (30) Lin, M.; DiVito, M. M.; Merajver, S. D.; Boyanapalli, M.; van Golen, K. L. Regulation of pancreatic cancer cell migration and invasion by RhoC GTPase and caveolin-1. *Mol. Cancer* **2005**, *4* (1), 21.
- (31) McHardy, L. M.; Sinotte, R.; Troussard, A.; Sheldon, C.; Church, J.; Williams, D. E.; Andersen, R. J.; Dedhar, S.; Roberge, M.; Roskelley, C. D. The tumor invasion inhibitor dihydromotuporamine C activates RHO, remodels stress fibers and focal adhesions, and stimulates sodium-proton exchange. *Cancer Res.* **2004**, *64* (4), 1468–1474.
- (32) To, K. C.; Loh, K. T.; Roskelley, C. D.; Andersen, R. J.; O'Connor, T. P. The anti-invasive compound motuporamine C is a robust stimulator of neuronal growth cone collapse. *Neuroscience* **2006**, *139* (4), 1263–1274.
- (33) Hannun, Y. A.; Obeid, L. M. Principles of bioactive lipid signalling: lessons from sphingolipids. *Nat. Rev. Mol. Cell Biol.* **2008**, *9* (2), 139–150.
- (34) Borselli, D.; Blanchet, M.; Bolla, J. M.; Muth, A.; Skrubber, K.; Phanstiel, O.; Brunel, J. M. Motuporamine derivatives as antimicrobial

agents and antibiotic enhancers against resistant Gram-negative bacteria. *ChemBioChem* **2017**, *18* (3), 276–283.